Experimental and Molecular Pathology 111 (2019) 104314

Contents lists available at ScienceDirect

Experimental and Molecular Pathology

journal homepage: www.elsevier.com/locate/yexmp

Cervical cancer patients that respond to chemoradiation therapy display an intense tumor infiltrating immune profile before treatment

Patrícia Rocha Martins[a,1], Christina Monerat Toledo Machado[a,1], Sarah Abreu Coxir[a], Adriana Jacaúna de Oliveira[a], Thayse Batista Moreira[a], Larissa Soares Campos[a], Romildo Alcântara[a], Sálua Oliveira Calil de Paula[a], Paulo Guilherme de Oliveira Salles[a], Kenneth J. Gollob[a,b,**,2], Wagner Carlos Santos Magalhães[a,*,2]

[a] Mário Penna Institute, Center for Teaching and Research, Belo Horizonte, MG, Brazil
[b] AC Camargo Cancer Center, Center for International Research, Translational Immuno-oncology Group, São Paulo, SP, Brazil

A B S T R A C T

Cervical cancer (CC) is a major cause of death and suffering to women globally with 570,000 new cases in 2017. It disproportionately affects those living in resource-constrained countries such as Brazil, with 90% of the deaths from CC happening in low and middle-income countries. Early detection is still the best strategy for improving response to therapy and survival and cases detected in advanced stages show variable response rates to the standard chemoradiation therapy protocols. Both the genetic landscape and the immune status of patients can dramatically affect cancer progression and response to therapy, as well as disease recurrence. Here we performed a comprehensive sequencing analysis using the cancer gene panel - Ion AmpliSeq™ Cancer hotspot Panel V2 CHPv2, as well as determined the immune infiltrate composition of a group of locally advanced CC patients with the goal of identifying genetic and immune characteristics associated with a clinical response to therapy. The expression levels of $CD68^+$ tumor-associated macrophages (TAMs) and $CD8^+$ tumor-infiltrating lymphocytes (TILs), as well as the immune checkpoint molecules PD-1, PD-L1 and PD-L2 in stroma and in tumor regions were analyzed by immunohistochemistry (IHC). The HPV infection status with high-risk strains was also determined. Twenty-one samples from patients with squamous cell carcinoma segregated into responder (11) and non-responder (10) groups according to standard chemoradiation therapy response were studied. Our findings indicate that responder patients showed an increase of an inflammatory tumor micro-environment as indicated by higher numbers of $CD8^+$ and $PD\text{-}L2^+$ TILs, as well as higher expression of PD-L1 immunoreactive area, as compared to the non-responder group. Additionally, our results demonstrate a correlation between the number of gene mutations and $PD\text{-}L2^+$ TILs in the responder group. The genes PIK3CA and KDR/VEGFR were the most mutated genes, corroborating past findings. Together, these findings indicate an inflammatory tumor microenvironment present in patients that will respond to future chemoradiation treatment as compared to those that will not. This points to possible future predictors of response to therapy in CC patients.

1. Introduction

Cervical cancer (CC) is the 4th most common cancer among women worldwide, with > 520,000 new cases being diagnosed every year. It represents 8% of all female cancer cases (Cancer Research UK, 2019). The majority is in resource-constrained environments such as Africa (Central and West) and Latin American (Jemal et al., 2011). In Brazil, according to the National Institute of Cancer (INCA), CC is the third most frequent tumor in the female population, behind breast and colorectal cancer, and the fourth leading cause of cancer deaths. The north region is responsible for the majority of the cases (INCA 2019).

Human papillomavirus (HPV) is the main cause of CC. Among > 200 genotypes of HPVs identified, only a few are responsible for most of the disease burden. The last International Classification Agency for Research on Cancer (IARC) defined 12 HPV strains as carcinogenic in humans, including HPVs 16, 18, 31, 33, 35, 39, 45, 51, 52, 56, 58, and 59 (Serrano et al., 2018). It's known that persistent infection with high risk HPV types 16 and 18 can cause genetic changes in cervical cells involved in cancer development and tumor progression mainly due to the action of viral oncogenes E6 and E7, which interact and inhibit the activity of cell cycle regulatory system components, represented by p53 (E6 target) and Rb (E7 target) (Borlu et al., 2016). Furthermore, the integration of HPV in the human genome may also contribute to genetic aberrations and gene expression modulation,

* Correspondence to: Wagner C. Santos Magalhães, Núcleo de Ensino e Pesquisa – NEP, Instituto Mario Penna, Rua Gentios, 1420, Belo Horizonte, MG 30380-472, Brazil.
** Correspondence to: Kenneth J. Gollob, International Research Center, A.C.Camargo Cancer Center, Rua Taguá 440, São Paulo, SP 01508-010, Brazil.
E-mail addresses: kenneth.gollob@accamargo.org.br (K.J. Gollob), wagner.magalhaes@mariopenna.org.br (W.C.S. Magalhães).
[1] These authors equally contributed to the present article.
[2] These authors equally contributed to the present article.

https://doi.org/10.1016/j.yexmp.2019.104314
Received 12 April 2019; Received in revised form 13 September 2019; Accepted 18 September 2019
Available online 22 October 2019

leading to cervical cell carcinogenesis (Das et al., 2016). Previous studies revealed that several genetic and epigenetic events play an important role in the CC carcinogenesis, like loss of heterozygosity, copy number alterations, tumor suppressor gene inactivation or oncogene activation (Cancer Genomic Atlas Research Network, 2017).

Detection of CC in the primary stages and beginning treatment as soon as possible are essential for the best prognosis (Denny, 2012). When patients present locally advanced non-metastatic disease, the standard treatment consists of platinum-based chemotherapy and radiotherapy sessions (Diaz-Padilla et al., 2013). New therapeutic approaches have arisen following a better understanding of the immune system role in cancer progression and pathogenesis. These studies include immunotherapeutic strategies such as immune checkpoint inhibitors alone or in combination with chemotherapy (Gadducci and Guerrieri, 2017).

An increased number of tumor-infiltrating lymphocytes (TILs) with cytotoxic and inflammatory phenotypes correlates with better outcome in many human cancers (Gooden et al., 2011). However, T cell responses against tumor cells can be inhibited through the engagement of immune checkpoint receptors expressed on the T cells surface, such as cytotoxic T lymphocyte-antigen 4 (CTLA-4) and programmed cell death (PD-1) (Francisco et al., 2009). The interaction between PD-1 on T cells and the programmed-death ligand (PD-L) 1 and 2 on the tumor cells or macrophages surface, inhibits T cell proliferation and increases Treg cell numbers, thus resulting in T cell functional inhibition and consequently pro-tumoral effects (Pardoll, 2012). Immunotherapy treatment via checkpoint inhibitors has proven effective at restoring anti-tumor function of TILs. Identification and characterization of factors that contribute to the immunosuppressive CC microenvironment such as dysfunction of genes and T cells, may be very important in trying to predict which patients will most benefit from this therapeutic strategy.

One of the key indicators associated with response to therapy and disease progression in human cancer is the genetic landscape as determined by mutations of key genes related to cancer development, progression and severity (Berger et al., 2018). In addition, higher mutational burden seems to be associated with more intense TILs and better responses to immune checkpoint inhibitor therapy (Thorsson et al., 2018). Here, we used the Ion AmpliSeq™ Cancer hotspot Panel (V2CHPv2), which is a panel of genomic “hot spot” regions that are frequently mutated in 50 oncogenes and tumor suppressor genes (Thermo Fisher, 2019).

Discovery of biomarkers that predict response to therapy remains a top priority in cancer medicine. Therefore, the ability to stratify patients through the identification of immunologic and genetic profiles could be key for enhancing survival through personalized treatment approaches by identifying non-responders, and thereby reducing the chance of these patients receive ineffective treatments. Here, using tumor biopsies taken before treatment began from patients that responded or not to chemoradiation therapy, we analyzed the local tumor immune profile composed of cellular expression of the T cell marker (CD8), macrophages (CD68) and immune checkpoints (PD-1, PD-L1, PD-L2), as well as a somatic mutation profile (target sequencing of 50 tumor suppressor and oncogenes that are commonly mutated in several types of cancers, (see Supplementary Material, Table 1) and HPV infection survey. Here, we demonstrated that before the treatment began, the eventual responder patients displayed an immunologically active inflammatory tumor microenvironment as compared to the non-responders, as evidenced by a higher number of $CD8^+$ and $PD\text{-}L2^+$ TILs, as well as a higher intensity of PD-L1 immunoreactive area, and an association with $PD\text{-}L2^+$ TILs expression and mutation number in the responder group.

2. Methods

2.1. Patients

Patients included in this retrospective study were women diagnosed with CC (squamous cell carcinoma) at Mario Penna Hospital between January 2014 to December 2016, clinically staged as IIB, IIIA or IIIB, according to the International Federation of Gynecology and Obstetrics (FIGO, 2019) criteria. Patients were submitted to chemotherapy and radiotherapy, and three to five months after the end of treatment were evaluated regarding the change in tumor load by physical examination and computer tomography imaging. Based on the findings, they were divided in two groups. The group of responders ($n = 11$) consisted of patients with complete response to therapy as determined by disappearance of all target lesions. The group of non-responders ($n = 10$) was composed of patients with partial response, progression of tumor or stable disease. The study was performed under approval #1.583.784 from the Ethical Committee at IMP.

2.2. Immunohistochemistry (IHC) assay

Cervical biopsies samples from these patients were retrieved from Pathology Department files. Paraffin blocks were cut into 4 μm thick sections and submitted to IHC labelling. Briefly, slides were deparaffinized in xylene and rehydrated in a graded alcohol series. The sections were submitted to microwave antigen retrieval using citrate buffer (pH = 6) or TRIS-EDTA solution pH = 9, for 10 min. Then endogenous peroxidase activity was inhibited by incubating the sections for 30 min in methanol containing 6% hydrogen peroxide. Next, the sections were incubated for 30 min with 2% normal albumin serum (Sigma, St. Louis, MO, USA) diluted in phosphate-buffered saline (PBS), and then incubated overnight at 4 °C with the following anti-human antibodies: anti-CD8, rabbit monoclonal (1:500, SP16, Cell Marque, Rocklin, USA); anti-PD-1, programmed death 1, mouse monoclonal (1:50, MA5–15780, Thermo Scientific, Rockford, USA); programmed death-ligand 1 (PD-L1), rabbit polyclonal (1:500, PA5–20343, Thermo Scientific, Rockford, USA); anti-CD273, programmed death-ligand 2 (PD-L2), rabbit polyclonal (1:500, PA5–20344, Thermo Scientific, Rockford, USA) and anti-CD68, macrophage marker, rat monoclonal (1:50, ab53444, Abcam, Cambridge, England). Subsequently, the samples were incubated with the Hidef Detection HRP Polymer System (Cell Marque, Rocklin, CA, USA) and the immune reactions were visualized using 0.03% of 3–3′-diaminobenzidine (SIGMA) containing 0.5% H_2O_2 in 0.01 M PBS, pH 7.4. Sections were counterstained with Gill's Hematoxylin (SIGMA), dehydrated, and mounted using a synthetic medium. A negative control without the primary antibody was generated for each sample.

2.3. Morphometric analysis

To determine the cellular composition and immune status of the CC lesions, the expression of brown stained immune cells, indicated by positive signal (+) of anti-CD68 and anti-CD8 markers, as well as the expression of immune checkpoint molecules PD-1, PD-L1 and PD-L2 were assessed in consecutive histological CC sections from responder and non-responder patients. For the quantification of immune cell location within the tumor, two regions were differentiated: 1) tumor-rich region (*peri* and intra-tumor) characterized by the epithelial compartment, defined as malignant cell nests and the fibrous tissue present between malignant cells and 2) the stroma-rich region, characterized by the connective tissue only in the periphery of the sample.

Although CD68 marker is highly expressed by monocytes and tissue macrophages, it is also expressed to a lesser extent on other cells, such as dendritic cells, peripheral blood granulocytes and tumor stroma cells (fibroblasts and endothelial cells). Given that CD68 is a phagocytic marker, here we considered cells that had macrophage morphological characteristics and expressed this marker as Tumor Associated-

Table 1
Clinicopathological characteristics and HPV infection status.

Group	Sample code	Age	Histologic grade	Tumor grade	Tumor size (~cm)	Parametrial involvement	Lymph node status	Metastasis	Lymphovascular invasion	13 HR HPV
NR	15947	38	II	NA	7	Unilaterally affected	N0	M0	−	−
NR	13564	54	II	III-A	7	Unilaterally affected	N1	M1	+	+
NR	10151	39	II	III-B	10	Bilaterally affected	N1	M1	−	+
NR	4514	88	II	III-B	6	Bilaterally affected	N0	M0	−	−
NR	7026	60	II	III-B	7	Bilaterally affected	N1	M1	+	+
NR	14595	76	III	III-B	5	Bilaterally affected	N1	M1	−	+
NR	3131	56	−	II-B	7	Bilaterally affected	N0	M0	−	+
NR	13563	70	III	III-B	6	Unilaterally affected	NX	M0	+	+
NR	12550	78	II	III-B	4	Bilaterally affected	N1	M1	+	−
NR	12273	74	I	III-B	12	Bilaterally affected	NX	M0	−	+
R	12245	63	III	III-B	7	Bilaterally affected	N0	M0	−	+
R	15892	82	III	II-B	5	Bilaterally affected	N0	M0	−	−
R	5583	31	II	II-B	7	Bilaterally affected	N0	M0	−	+
R	18244	38	III	III-B	6	Bilaterally affected	N0	M0	+	+
R	3838	77	III	II-B	3	Unilaterally affected	NX	M0	−	+
R	6288	54	III	III-B	9	Bilaterally affected	N0	M0	−	−
R	13722	69	I	III-B	7	Bilaterally affected	NX	M0	−	+
R	10801	47	III	III-B	6	Bilaterally affected	NX	M0	−	+
R	6419	60	III	III-B	6	Bilaterally affected	N0	M0	−	−
R	11485	77	II	III-B	11	Bilaterally affected	N0	M0	−	+
R	11479	55	III	II-B	1	Unilaterally affected	N0	M0	−	+

* NR = Non-responders, R = Responders; NX, Regional lymph nodes cannot be assessed; N0, No regional lymph node metastasis; N1, Regional lymph node metastasis; MX, Distant metastasis cannot be assessed; M0, No distant metastasis; M1, Distant metastasis; (FIGO, 2015). The symbols + and - signify presence or absence of Lymphovascular invasion and positive or negative for the 13 high-risk HPV types.

Macrophages (TAMs). For quantification of $CD68^+$ macrophages, the counting involved 10 randomly selected fields using a light microscope NIKON at 400× magnification (total area of 2.2 mm^2).

For CD8, PD-1, PD-L1 and PD-L2 protein expression in tumor-infiltrating lymphocytes (TILs) and other mononuclear and polymorphonuclear cells expressing PD-1, PD-L1 and PDL2, the counting was performed under a light microscope at 1000× magnification, in 10 randomly selected fields of each region per section (total area of 0.38mm^2). The criteria to positive cells was brown colour in both cytomembrane and/or cytoplasm.

Density of cells expressing PD-1, PD-L1/2 was also determined by measuring the percentage of total immunoreactive area (stroma and tumor), using the *ImageJ analysis software* (imagej.nih.gov/ij/). The evaluated area comprised 3 randomly selected fields using a light microscope NIKON at 400× magnification from a single histological section per patient. The average of total area analyzed was 180 mm^2 per patient. All sample analyses were made by two observers in a blinded manner.

For PD-L1 and PD-L2 expression in cancer cells, we chose the nests of CC and then calculated the proportion of positive cells following the score as presented by Reddy et al. (2017). Immunoreactive cytomembrane and cytoplasm or both were positive criteria. The cancer cells were evaluated as: 1) negative (score = 0, 0% of positive cells and 0% of intensity); 2) low-positive (score = 1A, < 50% of positive cells and 1^+, 2^+ and/or 3^+ of intensity); 3) positive (score = 2A, > 50% of positive cells and 1^+ of intensity); and 4) strong positive (score = 2B, > 50% of positive cells and 2^+ and/or 3^+ of intensity). The score percentage was used for comparisons among the groups. The correlations between the expression of these proteins and clinical histopathological parameters and molecular investigation were analyzed.

2.4. DNA extraction

DNA was extracted from FFPE samples using the AllPrep® DNA/RNA FFPE kit (Qiagen Cat No./ID: 80234) according to the manufacturer's instructions. The measurement of nucleic acid purity and quantification were accessed by NanoVue spectrophotometer (GE Healthcare Life Sciences) and Qubit® 2.0 Fluorometer with the Qubit® dsDNA HS Assay kit (Life Technologies), respectively. DNA was stored at −20 °C.

2.5. HPV infection

All samples were tested for the 13 high-risk HPV types (16, 18, 31, 33, 35, 39, 45, 51, 52, 56, 58, 59, and 68), using the kit 13 High Risk HPV PCR Real Time, HybriBio (China, lot: 20160601). The kit has a viral type-specific probes in the E6 gene. Briefly, H13 has two labeled probes, one for internal control for DNA adequacy (by detecting human beta-globin) and other for the detection of HPV DNA. Each probe consists of an oligonucleotide labeled with a reporter fluorophore at the 5'end and a quencher fluorophore at the 3'end. The primer extension and replication are performed by the enzyme Taq-polymerase. When hybridization occurs in the presence of specific viral DNA, a fluorescence signal is emitted and intensified at each PCR cycle and captured by the equipment. In this study we used the Real Time 7500 Applied Biosystems PCR.

2.6. Library preparation and sequencing

DNA libraries were carried out by using the panel AmpliSeq™ Cancer hotspot (V2CHPv2). All Amplicon libraries, Emulsion PCR and enrichment were prepared on the Ion Chef system using the Ion AmpliSeq Chef DL8 Kits (Thermo Fisher Scientific) according to the manufacturer's instructions. Lastly, sets of 8-pooled samples were loaded on an Ion 316 V2 chip and, finally, sequenced on the Ion PGM sequencing platform using the Ion Kit (Thermo Fisher Scientific), also performed on the Ion Chef System.

2.7. Bioinformatics framework

All sequences (*reads*) were aligned to the reference genome (hg19) and filtered by type of variant (e.g. Single Nucleotide Variants [SNVs], Multiple Nucleotide Variants and Indels) as well as variant effects (e.g. frameshift insertion, non-frameshift insertion, frameshift deletion, non-frameshift deletion, stop loss, missense, nonsense, and unknown) by using Ion Report software (version 5.6). The Ion Torrent Variant Caller Plugin v5.6 was used to call all variants and filtered by the following criteria, $0.05 \leq$ Minor Allele Frequency ≤ 0.5, $0.01 \leq$ Allele

Frequency ≤ 1.0 and last, Coverage ≥ 100. In addition, all polymorphisms were visually inspected using IGV, (Robinson et al., 2011; Thorvaldsdottir et al., 2013).

2.8. Statistical analysis

All statistical analyses were performed at the R platform and GraphPad Prism (Graphpad Software Inc., San Diego, CA). Firstly, we tested the dataset distribution using the Shapiro test. Next, we tested the hypothesis (H_0) of no differences of the number (median) and interquartile range (25–75%) boxes of polymorphisms using Wilcoxon test. In addition, for immunohistochemical data, we used a non-parametric Mann-Whitney and Kruskal-Wallis followed by Dunn's multiple comparison test. The correlation analysis was performed using the Spearman test. The results are expressed by mean (±) std. error. Differences were considered statistically significant at $p < 0.05$.

3. Results

3.1. Patient clinicopathologic characteristics

This study included 21 women with locally advanced cervical cancer (International Federation of Gynecology and Obstetrics stages IIB - IIIB), classified as squamous cell carcinoma (SCC), composed of 11 responder and 10 non-responder patients to standard chemoradiation therapy. The average age of patients was 60.2 with no significant difference between the groups (Table 1). Among patients with response to therapy, 72.8% presented the histological classification of poorly differentiated (GIII), divided into tumor stages of IIB (36%) and IIIB (63%). The patients from the non-responder group were classified as 60% moderately differentiated (GII) with 70% stage IIIB tumors. The average tumor size was 7.1 cm in non-responders and 6.1 cm in responder patients. The parametrial involvement (X-squared test, $p = 0.9028$) and lymphovascular invasion (X-squared test, p-value = 0.25) did not show difference between the groups. The lymph node status and metastasis, in non-responders showed 20% NX, 30% N0, 50% N1 and half of the patients (50%) showed metastasis; whereas the responders showed 27% NX, 73% N0, and no patient presented metastasis (Table 1).

3.2. HPV analysis

We did not observe a difference between the numbers of non-responder (7 of 10/ 70%) and responder (8 of 11/ 73%) patients positive for HPV infection, however, it is important to reinforce that using the 13 high-risk HPV kit, only 13 HPV strains were tested (Table 1).

3.3. Responder patients display a more intense before treatment tumor immune microenvironment infiltrate than non-responder patients

To gain insights into the immunoregulatory environment in CC tumors before treatment began in eventual responder vs. non-responder patients, we determined the cellular composition and immune status of the CC lesions by IHC (Figs. 1 and 2). A higher number of $CD68^+$ tumor associated macrophages (TAMs) were observed in stroma (Fig. 1a) and fewer within the tumor (*peri*/intra-tumoral) regions. However, no difference in the number of TAMs was observed between the responder (3.76 ± 1.4) vs. non-responder (2.1 ± 0.4) in the stroma, nor between the responder (1.45 ± 0.23) vs. non-responder (1.4 ± 0.3) in the *peri*/intra-tumoral region (Fig. 1a').

$CD8^+$ tumor-infiltrating lymphocytes (TILs) were seen dispersed throughout all regions of CC samples (Fig. 1b). Although the number of $CD8^+$ TILs was higher in stroma than tumor regions, a pronounced number were seen inside the tumor. It's worth pointing out that lymphocytes outnumbered TAMs in the *peri*/intra-tumoral region. Importantly, quantitation of $CD8^+$ TILs in the stroma demonstrated a dramatic increase in responders (19.8 ± 3.23) vs. non-responders (5.5 ± 2.8). The same was seen in the *peri*/intra-tumoral region when comparing responders (8.9 ± 0.6) vs. non-responders (4.8 ± 1.3) (Fig. 1b'). Immunoreactivity of $CD8^+$ TILs were not identified in three samples of non-responder patients (30%). Importantly, while positive rates of $CD8^+$ TILs seem higher in positive HPV CC samples, no significant difference in the number of $CD8^+$ TILs was seen between HPV positive (8.0 ± 1.3) and negative (6.7 ± 2.6) patients (Supplemental Fig. 1a).

The expression of immune checkpoints by TILs and cancer cells are represented in Fig. 2. PD-1 was expressed by the stromal lymphocytes with a higher concentration at the periphery of the tumor (Fig. 2a). PD-1 expression by TILs was not significantly different between responder (6.9 ± 2.2) and non-responder (3.4 ± 0.6) groups in the stroma, nor between responder (2 ± 0.4) and non-responder (1.8 ± 0.3) in the *peri* / intra-tumoral regions (Fig. 2a'). The total area of immunoreaction to PD-1 was also equivalent between the responders (358 ± 53.3) and non-responders (259 ± 26.2, Fig. 2a"). The ratio of $CD8^+$/$PD\text{-}1^+$ demonstrated a higher number of $CD8^+$ TILs than $PD\text{-}1^+$, but no difference was observed between the responder (5.2 ± 1.3) and non-responder (3.7 ± 1.3) patients in stroma, nor between the responder (12.7 ± 7.2) and non-responder (5.9 ± 2.8) in the *peri*/intratumor regions. The higher relative proportion of $CD8^+$ TILs identified by the $CD8^+$/$PD\text{-}1^+$ ratio demonstrated that a minority population of $CD8^+$ TILs express PD-1 and perhaps other subpopulations of lymphocytes express this checkpoint marker (Supplemental Fig. 1b).

$PD\text{-}L1^+$ and $PD\text{-}L2^+$ TILs were observed in higher numbers in the stroma than inside the tumor (Fig. 2b and c). The increase of TILs expressing PD-L1 was observed between the stroma (5.3 ± 1.8) and *peri*/intra-tumoral (1.3 ± 0.22) regions in non-responders, but not between the responder vs. non-responder groups (Fig. 2b'). However, when the total (stroma and tumor) PD-L1 immunoreactive (IR) area was measured, a larger area in responder (222.8 ± 36.6) was observed when compared to non-responder (127.3 ± 16) patients (Fig. 2b").

We next assessed the proportion of CC cells expressing PD-L1 using a validated score (strong positive, positive, low positive and negative cells). Most responder patients (38%) were strong positive for PD-L1 and only 8% were negative, suggesting PD-L1 induction via an inflammatory response in CC, while 37% of non-responder CC cells expressed low-positive for PD-L1 (Fig. 2b"'). In both groups, the percentage of PD-L1 positivity was higher than 50%.

PD-L2 expression by TILs was higher in responder (3.7 ± 0.7) compared to non-responder (1.4 ± 0.3) patients in the stroma region (Fig. 2c'). However, no difference was seen between the total PD-L2 immunoreactive area between responders (549.2 ± 164.4) and non-responders (313.8 ± 106.3, Fig. 2c"). The proportion of CC cells expressing PD-L2 were 50% in responder patients, 29% positive, and only 7% low-positive or negative, while 41.8% of the non-responder patients were strong positive, 16.6% positive, and 25% low-positive or negative for PD-L2 (Fig. 2c"'). Quantification of polymorphonuclear (neutrophils and eosinophils) and mononuclear cells (monocytes, macrophages and possibly dendritic cells) expressing PD-1, PD-L1/2 was also performed (Supplemental Fig. 2). While differences between the regions (stroma and tumor) were observed, none was seen comparing responder vs. non-responder groups to these cell populations. Lastly, no differences were seen between the expression of PD-1 and $PD\text{-}L1/2^+$ TILs in HPV positive vs. negative patients (data not showed). Thus, these studies demonstrated a more intense immune infiltrate, exemplified by higher $CD8^+$ cells and expression of inflammatory response related molecules (PD-L1/2) in the responder when compared to the non-responder group.

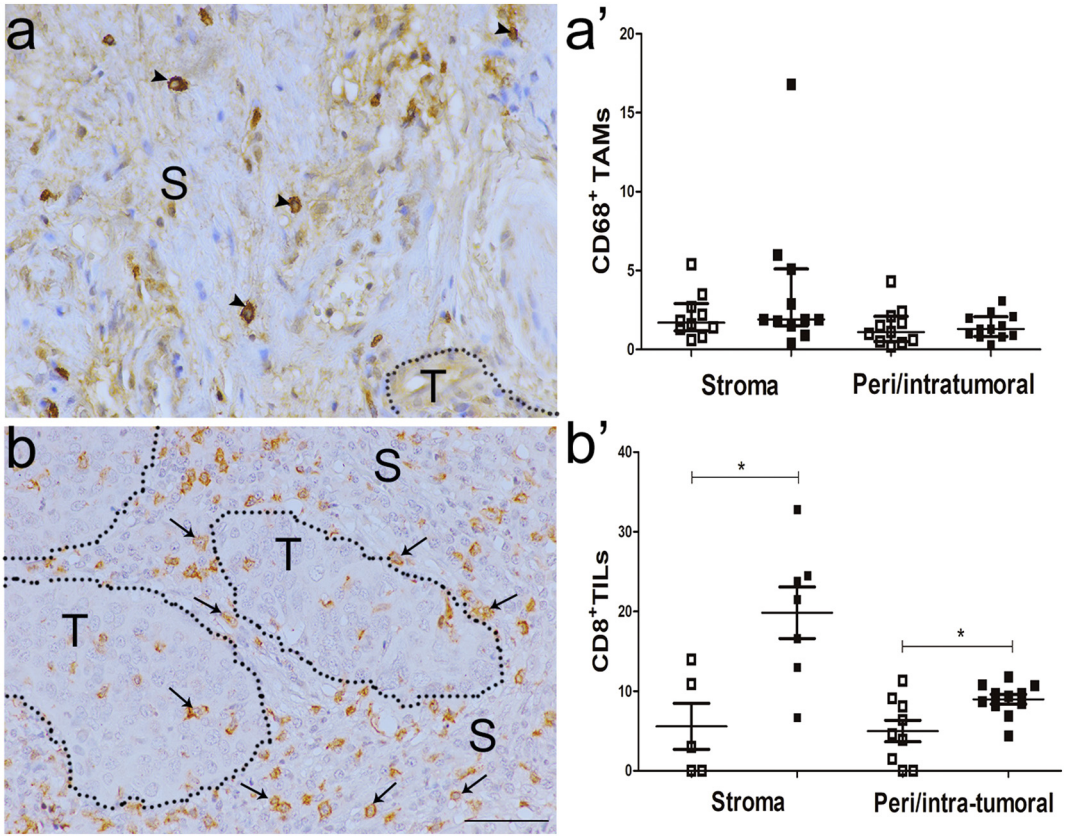

Fig. 1. Quantification of CD68$^+$ tumor-associated macrophages (TAMs) and CD8$^+$ tumor-infiltrating lymphocytes (TILs). In a and b are representative immunohistochemistry (IHC) images of brown stained immune cells ($^+$) indicating the protein expression of CD68$^+$ TAMs (a) and CD8$^+$ TILs (b) in human cervical cancer taken before treatment began at the time of diagnosis. The arrowhead indicates macrophages (a) and lymphocytes are represented by arrows (b). The regions are represented by (T) for Tumor and (S) for Stroma separated by black outlining (scale bar: 50 μm). In (a′), morphometric analysis of CD68$^+$ TAMs in stroma of responder (black squares) and non-responder (white squares) patients to chemoradiotherapy. No difference between the groups was observed considering $P < 0.05$. In (b′), quantification analysis showed the increase number of CD8$^+$ TILs in responder patients compared to non-responders in both, the stroma and *peri*/intratumoral regions. Note that individuals are represented by different symbols: □ represents the non-responder and ■ represents responder patients after chemoradiotherapy. * P < 0.05. (For interpretation of the references to colour in this figure legend, the reader is referred to the web version of this article.)

3.4. Non-responder patients display correlations of cell populations with inhibitory checkpoints consistent with an immunosuppressive tumor microenvironment as compared to the responder group

To gain insights into possible immunosuppressive or activated tumor microenvironments in the non-responder and responder groups, we performed a correlation analysis between the individual cell populations studied and the checkpoint molecules PD-1, PD-L1 and PD-L2. This analysis revealed a strong positive correlation between CD68$^+$ TAMs and PD-1$^+$ TILs (Fig. 3a, $r = 0.90$, $p = 0.001$), in the non-responder group and not in the responders in the tumor region (Fig. 3b). No significant correlations were seen for PD-L1 with CD68$^+$ TAMs in either group (Fig. 3c and d).

Moreover, a negative correlation was seen between the number of CD8$^+$ TILs and PD-1 in the stroma (Fig. 3e, $r = 0.94$, $p = 0.016$) or PD-L1 (Fig. 3g, $r = 0.72$, $p = 0.040$) expressing TILs in the non-responders in the tumor region, and not in the responders (Fig. 3f and h). Thus, potentially suppressive checkpoint molecules are positively associated with TAMs and negatively associated with CD8 cells in non-responding patients indicating a possible suppressive immune environment.

3.5. Gene sequencing of frequently mutated genes in cancer

To gain insights into possible associations between commonly mutated cancer related genes and the immune response and response to therapy, we performed NGS sequencing of our samples using the Ion AmpliSeq™ Cancer Hotspot Panel v2 panel. This panel uses 207 amplicons covering about 2800 COSMIC mutations from 50 oncogenes and tumor suppressor genes. We found 31 polymorphisms (13 Missense, 1 Nonsense, 7 Unknown and 10 Synonymous) in 19 genes, which comprises 29 Single Nucleotide Polymorphism (SNPs) and 2 short insertions/deletions (INDELS). Upon analysis of the responder vs. non-responder groups, it was apparent that the number of polymorphisms between the two groups was similar (Fig. 4).

Upon further analysis, we observed 9 private variants in the non-responder group (2 Missense, 1 Nonsense, 1 Unknown and 5 Synonymous) and 7 in the responder (5 Missense, 0 Nonsense, 1 Unknown and 1 Synonymous).

The most altered genes were PIK3CA ($n = 5$, 16%), KDR ($n = 3$, 9.6%) and MET (n = 3, 9.6%), with other genes bearing few polymorphisms. These three genes hold 35% of all variations, and more specifically, 35.7% of all non-synonymous observed polymorphisms (Fig. 5 - TOP). Our results are consistent with previous results in breast (Muller et al., 2016) and ovarian cancer (Sakai et al., 2017).

To evaluate how the polymorphisms found were able to discriminate between responder and non-responder groups, we generated a cluster heatmap. The analysis demonstrated that the polymorphisms did not segregate the responder and non-responders into distinct clades (Fig. 5, bottom left).

To investigate a possible relationship between the number of mutations and the immune profiles identified via immunohistochemistry analysis of the tumors, we performed a series of correlation analysis

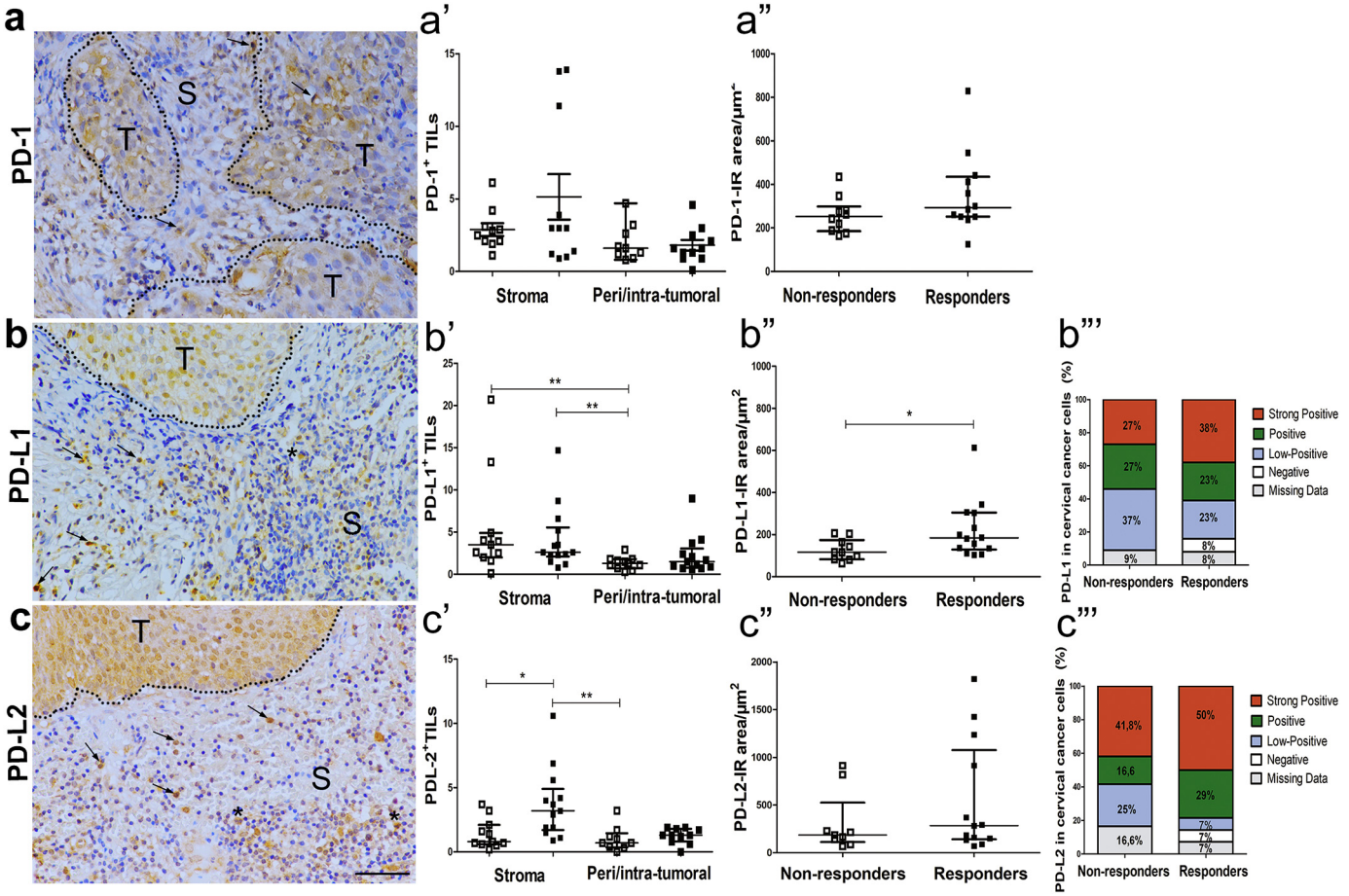

Fig. 2. Quantification of tumor-infiltrating lymphocytes (TILs) expressing PD-1, PD-L1 and PD-L2 immune checkpoints. a, b and c are representative immunohistochemistry (IHC) images of brown stained immune cells ($^+$) indicating the protein expression of PD-1 (a), PD-L1 (b) and PD-L2 (c) markers in human cervical cancer samples taken before treatment at the time of diagnosis. Lymphocytes are represented by arrows and polymorphonuclear cells indicated by asterisks. The regions are represented by (T) of Tumor and (S) of Stroma separated by black outlining (scale bar: 50 µm). In (a′), morphometric analysis of PD-1$^+$ TILs in the stroma and *peri*/intra-tumoral regions and (a″) immunoreactive (IR) area of PD-1/µm^2 in responder (black squares) and non-responder (white squares) patients. No difference between the groups was observed considering $P < 0.05$. In (b′), quantification analysis showed the increased number of PD-L1$^+$ TILs in the stroma compared to *peri*/intra-tumoral region in non-responder patients and increased number of PD-L1$^+$ TILs in the stroma of responder compared to *peri*/intra-tumoral region of non-responder patients ($P < 0.01$). In (b″), morphometric analysis showed the increased PD-L1-IR/µm^2 area (stroma and tumor regions) in responders compared to non-responders and in (c′), increased number of PD-L2$^+$ TILs in responder compared to non-responder patients in the stroma region. In (b‴) and (c‴), percentage of patients that exhibited different PD-L1 and PD-L2 protein expression levels (negative, low-positive, positive or strong positive) by cervical cancer cells in 21 samples of responder and non-responder patients. Note that individuals are represented by different symbols: □ represents non-responder patients and ■ represents responder patients to chemoradiotherapy. * $P < 0.05$, ** $P < 0.01$. (For interpretation of the references to colour in this figure legend, the reader is referred to the web version of this article.)

between the number of mutations and the immune indicators. This analysis showed a correlation between the number of mutations and PD-L2$^+$ TILs in the tumor region ($r = 0.67$) with a significant *p*-value ($p = 0.033$) for the responder group (Fig. 6b), but not for the non-responders ($r = 0.16$ and $p = 0.689$, Fig. 6a).

4. Discussion

In this study, we investigated the tumor immune and genetic profiles, as well as HPV infection status, before treatment began in a group of CC patients separated into responder vs. non-responder patients to chemoradiotherapy treatment. Given the clear role the immune response can have in control of cancer and response to therapy, we examined the number of TAMs (CD68), CD8 T cells, and the down modulatory checkpoints PD-1, PD-L1 and PD-L2, as well as intensity of expression of PD-L1 and PD-L2, in both the stroma and tumor regions. Our findings indicate that the responder patients showed a more intense inflamed profile, which may contribute to anti-tumor immunity and eventual response following chemoradiotherapy. In addition, these profiles may serve as predictive markers for patients that will respond to therapy.

Given the importance of CD8 T cells in the induction of anti-tumor immune responses, we investigated the number of CD8$^+$ cells in tumor biopsies of the responder and non-responder patients before treatment began. The patients that responded to chemoradiotherapy displayed a higher infiltration of CD8$^+$ T cells in the stroma and inside the tumor than the non-responders (Fig. 1). Earlier studies demonstrated CD8$^+$ cells concentrated at the tumor invasive margin in CC, suggesting a defect of T lymphocyte infiltration in these patients (Meng et al., 2018). Analysis of histological tumor sections by Chen and Mellman (2017) defined three basic immune profiles correlated with distinct responses to immunotherapy. First, the immune-inflamed phenotype, is characterized by high infiltration of CD8$^+$ and CD4$^+$ cells in the tumor parenchyma and PD-L1 staining in TILs and tumor cells; the second profile, immune-excluded phenotype, presenting immune cells that are retained in the stroma, but that do not penetrate inside the tumor; and the last one, the immune-desert phenotype, which is characterized by a paucity of T cells and a non-inflamed microenvironment (Herbst et al.,

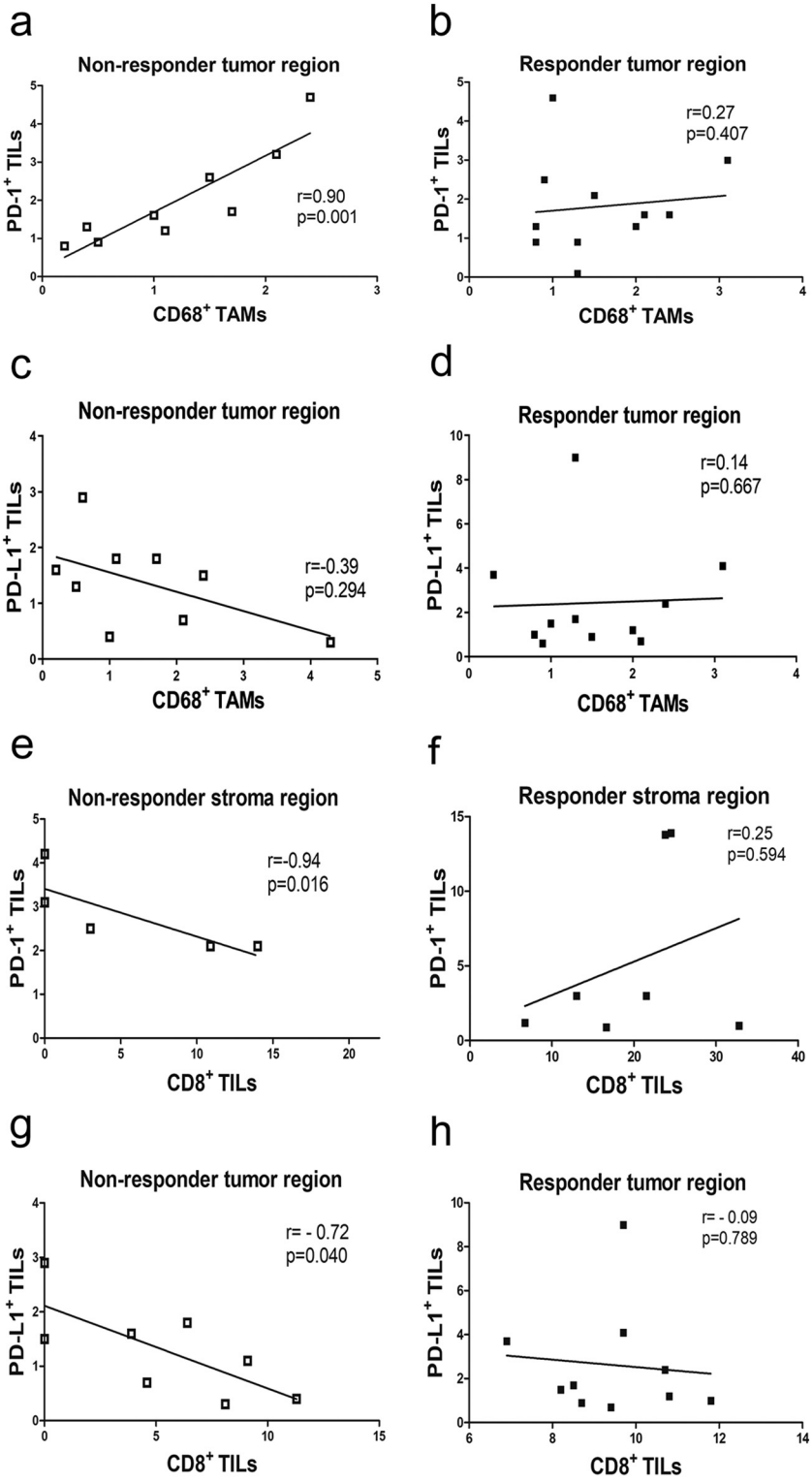

Fig. 3. Correlation analysis between immune cells of non-responder and responder patients. In (a), spearman test revealed a positive correlation between CD68+ TAMs and TILs expressing PD-1 ($n = 9$, $r = 0.90$, $p = 0.001$) in non-responder tumor region, and no correlation in the responder tumor region (b). In (c and d) PD-L1+ TILs did not show a significant correlation (n = 9, $r = -0.39$, $p = .294$) in non-responders or in responders ($n = 11$, $r = 0.14$, $p = 0.667$). In (e), a negative correlation between CD8+ TILs and PD-1+ TILs ($n = 5$, $r = 0.94$, $p = 0.016$) in the stroma region, and in (g) between CD8+ TILs and PD-L1+ TILs ($n = 8$, $r = 0.72$, $p = 0.040$) in non-responder tumor region, in contrast to the responder group (f and h). Note that individuals are represented by different symbols: □ represents the non-responder patients and ■ represents responder patients after chemoradiotherapy. Significance was considered when $p < 0.05$.

2014). Our results suggest that CC patients can exhibit the immune-inflamed or excluded profile, but patients that respond to therapy display a higher inflamed phenotype than those that do not. Ock et al. (2016) found that some patients displayed a high number of CD8 and PD-L1 staining cells, while others presented none or few cells staining positive for these markers. Moreover, the highest number of $CD8^+$ TILs were strongly associated with an improved prognosis in several other studies in different solid tumors (Liakou et al., 2007; Katz et al., 2013; Dieci et al., 2015; Ock et al., 2016; Li and Xu, 2016).

More recently, $CD8^+$ cell infiltration was investigated as a biomarker of response to PD-1/PD-L1 monotherapy in a cohort of advanced solid tumor patients. Using a radiomic signature to classify the patients as either immune-inflamed tumor (with dense $CD8^+$ TILs) or immune-desert (with low $CD8^+$ TILs) phenotypes, a clear correlation between response to therapy and overall survival and the immune-inflamed tumor phenotype was demonstrated (Sun et al., 2018). These findings reinforce the concept that $CD8^+$ T cell infiltration is a robust biomarker for the identification of patients that will respond to

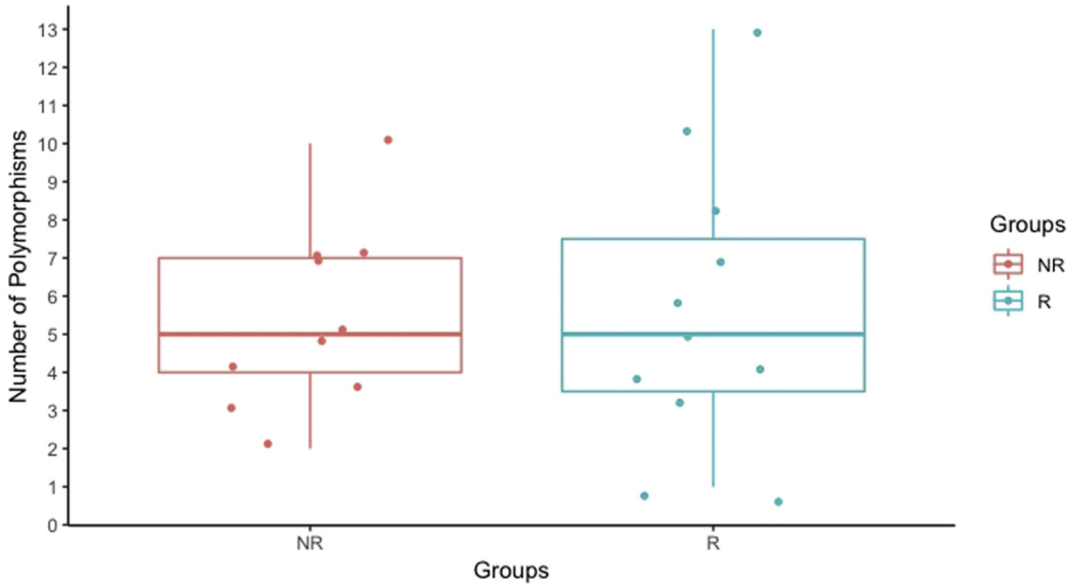

Fig. 4. Box plot of polymorphisms between Responders (R) and Non-Responders (NR). DNA was purified from FFPE samples and prepared as described in Materials and Methods, using the same samples used for determination of the immune profile studies. $n = 10$ for non-responder and n = 11 for the responder group. The graphs represent the median and interquartile range (25–75%) boxes.

immunotherapy. In addition, the negative correlation between higher levels of PD-1 or PD-L1 expressing TILs and lower levels of $CD8^+$ TILs in the non-responder group, together with the correlation between $CD68^+$ TAMs and the negative regulatory molecules PD-1 (Fig. 3), support a suppressive tumor microenvironment in non-responders in comparison to the responder group.

Moreover, the increased expression of PD-L1 and PD-L2 in TILs and tumor cells in the responder patients together with the increased $CD8^+$ TILs, indicates an immune-inflamed phenotype as compared to the non-responder patients. Indeed, earlier studies demonstrated that the clinical responses to anti-PD-1/PD-L1 therapy occur most often in patients with inflamed tumors (Garon et al., 2015; Ayers et al., 2018). In

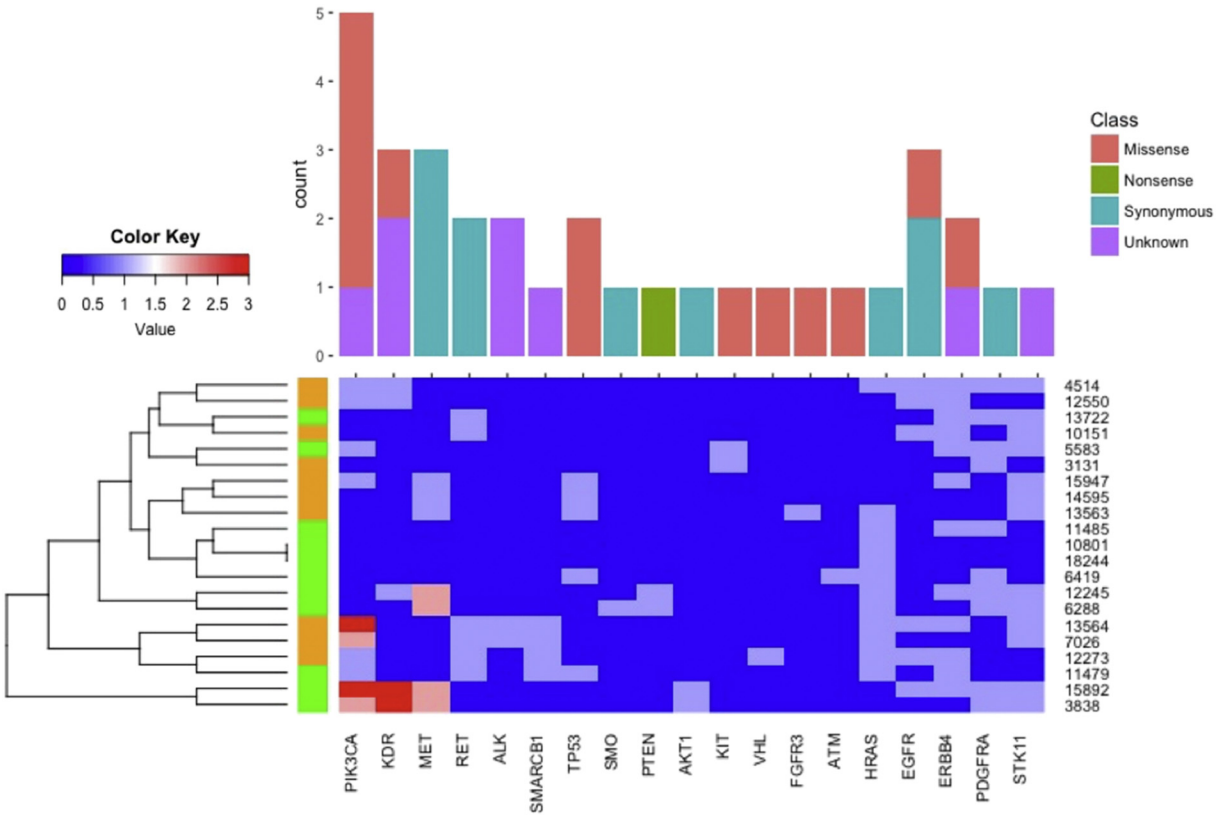

Fig. 5. Polymorphism overview. Bar plot overview of polymorphism classes (Missense, Nonsense, Synonymous and Unknown) distribution along 19 genes (TOP), and a Heatmap, with the result of that distribution between the groups (Non-responders - orange and Responders - green) (BOTTOM). (For interpretation of the references to colour in this figure legend, the reader is referred to the web version of this article.)

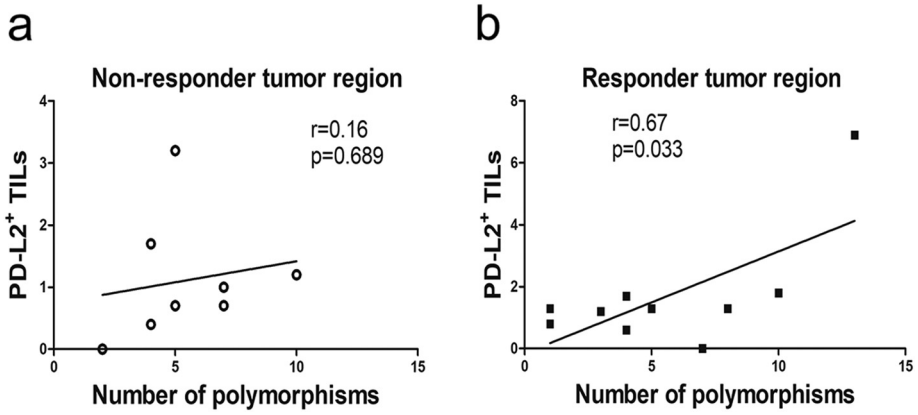

Fig. 6. Correlation analysis between the number of mutations and PD-L2$^+$ TILs. (a) There is no correlation in non-responder group (r = 0.68, p-value = .16) and (b) a positive correlation between number of mutations and PD-L2$^+$ TILs in the tumor region of responder patients (r = 0.67, p-value = .033).

recognition of these findings and others, the FDA has granted accelerated approval for the treatment of patients with PD-L1$^+$ advanced CC using pembrolizumab (Frenel et al., 2017; OncoLive, 2019).

Furthermore, the correlation between CD8$^+$ TILs and HPV was investigated. In this study, HPV was detected in most of the CC samples (73% of responders and 70% of non-responders). Bashaw et al. (2017) have identified a relationship between HPV infection and antigen persistence with the number of CD8$^+$ TILs, however, in our study no difference was observed between the rates of CD8$^+$ TILs in HPV positive and HPV negative samples. Although the expression of PD-L1 and PD-L2$^+$ TILs appeared higher in HPV positive patients, no statistically significant difference was observed between the groups. An association between HPV infection and PD-1/PD-L1 expression was described in several other studies (Yang et al., 2013; Mezache et al., 2015; Liu et al., 2017; Meng et al., 2018), with Liu et al. (2017) describing a lymphocyte dysfunction related to the over-expression of PD-L1. Nevertheless, our results demonstrated that HPV negative patients (negative for the 13 high risk strains tested in our PCR) responding to therapy showed higher numbers of PD-L1$^+$ TILs, suggesting that HPV infection is not the unique mechanism accountable for the over-expression of PD-L1 in CC patients and may not always induce a suppressive response. Together, these results indicate that the relationship between HPV and PD1/PDL1 pathway deserves further investigation.

We also investigated the association between HPV infection and number of polymorphisms. No correlation was found between the number of somatic mutations and HPV infection. Our results are consistent with Cox et al. (2013), who did not find association between number of somatic mutations and HPV-16 and HPV-18 strains infection.

Concerning the polymorphisms in specific genes, the most mutated gene was PIK3CA (n = 5, 16%), which is considered a significantly mutated gene (SMG) in CC. This gene is responsible for coding the catalytic subunit of phosphatidylinositol 3-kinase (PI3K). Mutations in PIK3CA lead to altered production of the catalytic subunit (p110α) of phosphatidylinositol 3-kinase (PI3K), leading the PI3K pathway to signal without regulation, and subsequent uncontrolled cell growth, proliferation and survival (Das et al., 2016). Our findings, even with a small number of patients, are in accordance with other works that reported a rate between 23 and 36% of mutations in PIK3CA in CC specimens. In addition, some authors correlated mutation in this pathway with higher rates of recurrence (Cox et al., 2013). Three specific missense mutations, E545K, E542K and E81K, suggest an APOBEC mutagenesis signature (Cancer Genome Atlas Research Network, 2017).

The second gene most mutated was KDR/VEGFR2 (n = 3, 9.6%), which is the primary receptor mediating VEGF-A activity on endothelial cells enhancing proliferation, migration and survival (Terman et al., 1992; Waltenberger et al., 1994; Gerber et al., 1998; Jia et al., 2004). In neoplastic development and progression, Tyrosine Kinase Receptors (RTKS) are commonly deregulated and excessive phosphorylation sustains signal transduction pathways leading to an activated state and tumor growth, progression, proliferation, differentiation, inhibition of apoptosis, metastasis and angiogenesis (Longatto-Filho et al., 2009). Here, we found in our sequencing results a missense non-synonymous mutation, rs1870377, with a tolerated SIFT score and minor allele frequency (MAF) of 0.2119 according to the 1000 genomes project, but with no ClinVar database information. This SNP was previously reported in a study with glandular odontogenic cyst (de Siqueira et al., 2017).

Combining the findings of the mutation number in the responder vs. non-responder groups with the immune profile data, a positive correlation between the number of gene mutations and the number of PD-L2$^+$ TILs was seen in the responder group, and not in the non-responder group (Fig. 6). This may indicate a possible association between greater genomic instability and a more active immune response, while this cannot be affirmed with the number of samples used in this study.

In conclusion, our studies show that CC patients that go on to respond to chemoradiation therapy display a more intense immune inflamed phenotype characterized by a greater CD8$^+$ TILs and higher expression of PD-1, and PD-L1/2 as compared to the non-responder group. Importantly, the non-responder group showed a negative correlation between PD-1 expression and CD8$^+$ TILs, and a positive correlation between TAMs and PD-1 and PD-L1$^+$ TILs, consistent with a suppressed immune microenvironment. Moreover, an association between the number of mutations and PD-L2$^+$ TILs suggests further studies between specific gene mutations and immune activity in responder vs. non-responder CC patients. Thus, taken together, these studies demonstrate a potential role for early tumor immune activation and subsequent response to chemoradiation therapy and pave the way for further studies to investigate the molecular and immunoregulatory mechanisms behind these findings.

Declaration of Competing Interest

The authors declare that they have no conflict of interest.

Acknowledgements

We are grateful to Rosicléia Freitas de Cerqueira and all from Luxemburgo Hospital Pathology laboratory for their help with the FFPE blocks, as well as all clinicians of gynecology group of the Instituto Mario Penna involved in the project. We are also grateful to Ministry of Health (Pronon - SIPAR : 25000.159953/2014-18) and the Minas Gerais State Research Agency (FAPEMIG), which funded this study. The study and its participants also received funding and fellowships from the following Brazilian agencies: Brazilian National Research Council

(CNPq), Ministry of Education (CAPES), Ministry of Health (Pronon) and the Minas Gerais State Research Agency (FAPEMIG).

Appendix A. Supplementary data

Supplementary data to this article can be found online at https://doi.org/10.1016/j.yexmp.2019.104314.

References

Ayers, M., Nebozhyn, M., Cristescu, R., McClanahan, T.K., Perini, R., Rubin, E., Cheng, J.D., Kaufman, D.R., Loboda, A., 2018. Molecular profiling of cohorts of tumor samples to guide clinical development of Pembrolizumab as monotherapy. Clin. Cancer Res. doi. https://doi.org/10.1158/1078-0432.CCR-18-1316.

Bashaw, A.A., Leggatt, G.R., Chandra, J., Tuong, Z.K., Frazer, I.H., 2017. Modulation of antigen presenting cell functions during chronic HPV infection. Papillomavirus Res. (Amsterdam, Netherlands) 4, 58–65. https://doi.org/10.1016/j.pvr.2017.08.002.

Berger, O., Gronberg, B.H., Loge, J.H., Kaasa, S., Sand, K., 2018. Cancer patients' knowledge about their disease and treatment before, during and after treatment: a prospective, longitudinal study. BMC Cancer 18, 381. https://doi.org/10.1186/s12885-018-4164-5.

Borlu, A., Gunay, O., Balci, E., Sagiroglu, M., 2016. Knowledge and attitudes of medical and non-medical Turkish university students about cervical cancer and HPV vaccination. Asian Pac. J. Cancer Prev. 17, 299–303.

Cancer Genome Atlas Research Network, 2017. Integrated genomic and molecular characterization of cervical cancer. Nature 543, 378–384. https://doi.org/10.1038/nature21386.

Cancer Research UK, 2019. Cancer reports for the UK. https://scienceblog.cancerresearchuk.org/ accessed 02 April 2019.

Chen, D.S., Mellman, I., 2017. Elements of cancer immunity and the cancer-immune set point. Nature 541, 321–330. https://doi.org/10.1038/nature21349.

Cox, J.T., Castle, P.E., Behrens, C.M., Sharma, A., Wright, T.C.J., Cuzick, J., 2013. Comparison of cervical cancer screening strategies incorporating different combinations of cytology, HPV testing, and genotyping for HPV 16/18: results from the ATHENA HPV study. Am. J. Obstet. Gynecol. 208, 184.e1–184.e11. https://doi.org/10.1016/j.ajog.2012.11.020.

Das, P., Bansal, A., Rao, S.N., Deodhar, K., Mahantshetty, U., Shrivastava, S.K., Sivaraman, K., Mulherkar, R., 2016. Somatic variations in cervical cancers in Indian patients. PLoS One 11, e0165878. https://doi.org/10.1371/journal.pone.0165878.

de Siqueira, E.C., de Sousa, S.F., Franca, J.A., Diniz, M.G., Pereira, T.D.S.F., Moreira, R.G., Vargas, P.A., Gomez, R.S., Gomes, C.C., 2017. Targeted next-generation sequencing of glandular odontogenic cyst: a preliminary study. Oral Surg. Oral Med. Oral Pathol. Oral Radiol. 124, 490–494. https://doi.org/10.1016/j.oooo.2017.07.001.

Denny, L., 2012. Cervical cancer: prevention and treatment. Discov. Med. 14, 125–131.

Diaz-Padilla, I., Monk, B.J., Mackay, H.J., Oaknin, A., 2013. Treatment of metastatic cervical cancer: future directions involving targeted agents. Crit. Rev. Oncol. Hematol. 85, 303–314. https://doi.org/10.1016/j.critrevonc.2012.07.006.

Dieci, M.V., Criscitiello, C., Goubar, A., Viale, G., Conte, P., Guarneri, V., Ficarra, G., Mathieu, M.C., Delaloge, S., Curigliano, G., Andre, F., 2015. Prognostic value of tumor-infiltrating lymphocytes on residual disease after primary chemotherapy for triple-negative breast cancer: a retrospective multicenter study. Ann. Oncol. Off. J. Eur. Soc. Med. Oncol. https://doi.org/10.1093/annonc/mdv241.

Federation of Gynecology and Obstetrics criteria, 2019. https://www.figo.org/ (accessed 15 November 2017).

Francisco, L.M., Salinas, V.H., Brown, K.E., Vanguri, V.K., Freeman, G.J., Kuchroo, V.K., Sharpe, A.H., 2009. PD-L1 regulates the development, maintenance, and function of induced regulatory T cells. J. Exp. Med. 206, 3015–3029. https://doi.org/10.1084/jem.20090847.

Frenel, J.-S., Le Tourneau, C., O'Neil, B., Ott, P.A., Piha-Paul, S.A., Gomez-Roca, C., van Brummelen, E.M.J., Rugo, H.S., Thomas, S., Saraf, S., Rangwala, R., Varga, A., 2017. Safety and efficacy of Pembrolizumab in advanced, programmed death ligand 1-positive cervical Cancer: results from the phase Ib KEYNOTE-028 trial. J. Clin. Oncol. 35, 4035–4041. https://doi.org/10.1200/JCO.2017.74.5471.

Gadducci, A., Guerrieri, M.E., 2017. Immune checkpoint inhibitors in gynecological cancers: update of literature and perspectives of clinical research. Anticancer Res. 37, 5955–5965. https://doi.org/10.21873/anticanres.12042.

Garon, E.B., Rizvi, N.A., Hui, R., Leighl, N., Balmanoukian, A.S., Eder, J.P., Patnaik, A., Aggarwal, C., Gubens, M., Horn, L., Carcereny, E., Ahn, M.-J., Felip, E., Lee, J.-S., Hellmann, M.D., Hamid, O., Goldman, J.W., Soria, J.-C., Dolled-Filhart, M., Rutledge, R.Z., Zhang, J., Lunceford, J.K., Rangwala, R., Lubiniecki, G.M., Roach, C., Emancipator, K., Gandhi, L., 2015. Pembrolizumab for the treatment of non-small-cell lung cancer. N. Engl. J. Med. 372, 2018–2028. https://doi.org/10.1056/NEJMoa1501824.

Gerber, H.P., McMurtrey, A., Kowalski, J., Yan, M., Keyt, B.A., Dixit, V., Ferrara, N., 1998. Vascular endothelial growth factor regulates endothelial cell survival through the phosphatidylinositol 3′-kinase/Akt signal transduction pathway. Requirement for Flk-1/KDR activation. J. Biol. Chem. 273, 30336–30343.

Gooden, M.J.M., de Bock, G.H., Leffers, N., Daemen, T., Nijman, H.W., 2011. The prognostic influence of tumour-infiltrating lymphocytes in cancer: a systematic review with meta-analysis. Br. J. Cancer 105, 93–103. https://doi.org/10.1038/bjc.2011.189.

Herbst, R.S., Soria, J.-C., Kowanetz, M., Fine, G.D., Hamid, O., Gordon, M.S., Sosman, J.A., McDermott, D.F., Powderly, J.D., Gettinger, S.N., Kohrt, H.E.K., Horn, L., Lawrence, D.P., Rost, S., Leabman, M., Xiao, Y., Mokatrin, A., Koeppen, H., Hegde, P.S., Mellman, I., Chen, D.S., Hodi, F.S., 2014. Predictive correlates of response to the anti-PD-L1 antibody MPDL3280A in cancer patients. Nature 515, 563–567. https://doi.org/10.1038/nature14011.

Instituto Nacional de Câncer (INCA), 2019. https://www.inca.gov.br/numeros-de-cancer> accessed 15 November 2017.

Jemal, A., Bray, F., Center, M.M., Ferlay, J., Ward, E., Forman, D., 2011. Global cancer statistics. CA Cancer J. Clin. 61, 69–90. https://doi.org/10.3322/caac.20107.

Jia, H., Bagherzadeh, A., Bicknell, R., Duchen, M.R., Liu, D., Zachary, I., 2004. Vascular endothelial growth factor (VEGF)-D and VEGF-A differentially regulate KDR-mediated signaling and biological function in vascular endothelial cells. J. Biol. Chem. 279, 36148–36157. https://doi.org/10.1074/jbc.M401538200.

Katz, S.C., Bamboat, Z.M., Maker, A.V., Shia, J., Pillarisetty, V.G., Yopp, A.C., Hedvat, C.V., Gonen, M., Jarnagin, W.R., Fong, Y., D'Angelica, M.I., DeMatteo, R.P., 2013. Regulatory T cell infiltration predicts outcome following resection of colorectal cancer liver metastases. Ann. Surg. Oncol. 20, 946–955. https://doi.org/10.1245/s10434-012-2668-9.

Li, X., Xu, J.-X., 2016. A mathematical prognosis model for pancreatic cancer patients receiving immunotherapy. J. Theor. Biol. 406, 42–51. https://doi.org/10.1016/j.jtbi.2016.06.021.

Liakou, C.I., Narayanan, S., Ng Tang, D., Logothetis, C.J., Sharma, P., 2007. Focus on TILs: prognostic significance of tumor infiltrating lymphocytes in human bladder cancer. Cancer Immun. 7, 10.

Liu, C., Lu, J., Tian, H., Du, W.E.I., Zhao, L.I.N., Feng, J., Yuan, D., Li, Z., 2017. Increased expression of PD - L1 by the human papillomavirus 16 E7 oncoprotein inhibits anticancer immunity. pp. 1063–1070. https://doi.org/10.3892/mmr.2017.6102.

Longatto-Filho, A., Malheiro, L.F.G., Milanezi, F., Pinheiro, C., Baltazar, F., Schmitt, F.C., Montironi, R., 2009. Lymphatic vessel density in the normal-looking columnar epithelium adjacent to and distant from prostatic intraepithelial neoplasia and prostate cancer assessed in whole-mount sections. Anal. Quant. Cytol. Histol. 31, 269–275.

Meng, Y., Liang, H., Hu, J., Liu, S., Hao, X., Wong, M.S.K., Li, X., Hu, L., 2018. PD-L1 expression correlates with tumor infiltrating lymphocytes and response to neoadjuvant chemotherapy in cervical cancer. J. Cancer 9, 2938–2945. https://doi.org/10.7150/jca.22532.

Mezache, L., Paniccia, B., Nyinawabera, A., Nuovo, G.J., 2015. Enhanced expression of PD L1 in cervical intraepithelial neoplasia and cervical cancers. Mod. Pathol. 28, 1594–1602. https://doi.org/10.1038/modpathol.2015.108.

Muller, K.E., Marotti, J.D., de Abreu, F.B., Peterson, J.D., Miller, T.W., Chamberlin, M.D., Tsongalis, G.J., Tafe, L.J., 2016. Targeted next-generation sequencing detects a high frequency of potentially actionable mutations in metastatic breast cancers. Exp. Mol. Pathol. 100, 421–425. https://doi.org/10.1016/j.yexmp.2016.04.002.

Ock, C.-Y., Keam, B., Kim, S., Lee, J.-S., Kim, M., Kim, T.M., Jeon, Y.K., Kim, D.-W., Chung, D.H., Heo, D.S., 2016. Pan-cancer immunogenomic perspective on the tumor microenvironment based on PD-L1 and CD8 T-cell infiltration. Clin. Cancer Res. 22, 2261–2270. https://doi.org/10.1158/1078-0432.CCR-15-2834.

OncoLive, 2019. www.onclive.com/web-exclusives/fda-approvespembrolizumab-for-pdl1-cervical-cancer accessed 15 January 2019.

Pardoll, D.M., 2012. Immunology beats cancer: a blueprint for successful translation. Nat. Immunol. 13, 1129–1132. https://doi.org/10.1038/ni.2392.

Reddy, O.L., Shintaku, P.I., Moatamed, N.A., 2017. Programmed death-ligand 1(PD-L1) is expressed in a significant number of the uterine cervical carcinomas. 1. pp. 1–11. https://doi.org/10.1186/s13000-017-0631-6.

Robinson, J.T., Thorvaldsdottir, H., Winckler, W., Guttman, M., Lander, E.S., Getz, G., Mesirov, J.P., 2011. Integrative genomics viewer. Nat. Biotechnol. https://doi.org/10.1038/nbt.1754.

Sakai, K., Ukita, M., Schmidt, J., Wu, L., De Velasco, M.A., Roter, A., Jevons, L., Nishio, K., Mandai, M., 2017. Clonal composition of human ovarian cancer based on copy number analysis reveals a reciprocal relation with oncogenic mutation status. Cancer Lett. 405, 22–28. https://doi.org/10.1016/j.canlet.2017.07.013.

Serrano, B., Brotons, M., Bosch, F.X., Bruni, L., 2018. Epidemiology and burden of HPV-related disease. Best Pract. Res. Clin. Obstet. Gynaecol. 47, 14–26. https://doi.org/10.1016/j.bpobgyn.2017.08.006.

Sun, R., Limkin, E.J., Vakalopoulou, M., Dercle, L., Champiat, S., Han, S.R., Verlingue, L., Brandao, D., Lancia, A., Ammari, S., Hollebecque, A., Scoazec, J.-Y., Marabelle, A., Massard, C., Soria, J.-C., Robert, C., Paragios, N., Deutsch, E., Ferte, C., 2018. A radiomics approach to assess tumour-infiltrating CD8 cells and response to anti-PD-1 or anti-PD-L1 immunotherapy: an imaging biomarker, retrospective multicohort study. Lancet. Oncol. 19, 1180–1191. https://doi.org/10.1016/S1470-2045(18)30413-3.

Terman, B.I., Dougher-Vermazen, M., Carrion, M.E., Dimitrov, D., Armellino, D.C., Gospodarowicz, D., Bohlen, P., 1992. Identification of the KDR tyrosine kinase as a receptor for vascular endothelial cell growth factor. Biochem. Biophys. Res. Commun. 187, 1579–1586.

Thermo Fisher Scientific, 2019. Ion AmpliSeq™ Cancer Hotspot Panel v2. https://www.thermofisher.com/order/catalog/product/4475346 accessed 02 April 2019.

Thorsson, V., Gibbs, D.L., Brown, S.D., Wolf, D., Bortone, D.S., Ou Yang, T.-H., Porta-Pardo, E., Gao, G.F., Plaisier, C.L., Eddy, J.A., Ziv, E., Culhane, A.C., Paull, E.O., Sivakumar, I.K.A., Gentles, A.J., Malhotra, R., Farshidfar, F., Colaprico, A., Parker, J.S., Mose, L.E., Vo, N.S., Liu, J., Liu, Y., Rader, J., Dhankani, V., Reynolds, S.M., Bowlby, R., Califano, A., Cherniack, A.D., Anastassiou, D., Bedognetti, D., Rao, A., Chen, K., Krasnitz, A., Hu, H., Malta, T.M., Noushmehr, H., Pedamallu, C.S., Bullman, S., Ojesina, A.I., Lamb, A., Zhou, W., Shen, H., Choueiri, T.K., Weinstein, J.N., Guinney, J., Saltz, J., Holt, R.A., Rabkin, C.E., Lazar, A.J., Serody, J.S., Demicco, E.G., Disis, M.L., Vincent, B.G., Shmulevich, L., 2018. The immune landscape of cancer. Immunity 48, 812–830.e14. https://doi.org/10.1016/j.immuni.2018.03.023.

Thorvaldsdottir, H., Robinson, J.T., Mesirov, J.P., 2013. Integrative genomics viewer

(IGV): high-performance genomics data visualization and exploration. Brief. Bioinform. 14, 178–192. https://doi.org/10.1093/bib/bbs017.

Waltenberger, J., Claesson-Welsh, L., Siegbahn, A., Shibuya, M., Heldin, C.H., 1994. Different signal transduction properties of KDR and Flt1, two receptors for vascular endothelial growth factor. J. Biol. Chem. 269, 26988–26995.

Yang, W., Song, Y., Sun, J., Wang, W., 2013. Increased expression of programmed death (PD)-1 and its ligand PD-L1 correlates with impaired cell-mediated immunity in high-risk human papillomavirus-related cervical intraepithelial neoplasia. https://doi.org/10.1111/imm.12101.